

Measurement of the $WW + WZ$ Production Cross Section Using the lepton + jets Final State at CDF II

T. Aaltonen,²⁴ J. Adelman,¹⁴ B. Álvarez González,^{12,w} S. Amerio,^{44b,44a} D. Amidei,³⁵ A. Anastassov,³⁹ A. Annovi,²⁰ J. Antos,¹⁵ G. Apollinari,¹⁸ A. Apresyan,⁴⁹ T. Arisawa,⁵⁸ A. Artikov,¹⁶ J. Asaadi,⁵⁴ W. Ashmanskas,¹⁸ A. Attal,⁴ A. Aurisano,⁵⁴ F. Azfar,⁴³ W. Badgett,¹⁸ A. Barbaro-Galtieri,²⁹ V. E. Barnes,⁴⁹ B. A. Barnett,¹ P. Barria,^{47c,47a} P. Bartos,¹⁵ G. Bauer,³³ P.-H. Beauchemin,³⁴ F. Bedeschi,^{47a} D. Beecher,³¹ S. Behari,¹ G. Bellettini,^{47b,47a} J. Bellinger,⁶⁰ D. Benjamin,¹⁷ A. Beretvas,¹⁸ A. Bhatti,⁵¹ M. Binkley,¹⁸ D. Bisello,^{44b,44a} I. Bizjak,^{31,dd} R. E. Blair,² C. Blocker,⁷ B. Blumenfeld,¹ A. Bocci,¹⁷ A. Bodek,⁵⁰ V. Boisvert,⁵⁰ D. Bortoletto,⁴⁹ J. Boudreau,⁴⁸ A. Boveia,¹¹ B. Brau,^{11,b} A. Bridgeman,²⁵ L. Brigliadori,^{6b,6a} C. Bromberg,³⁶ E. Brubaker,¹⁴ J. Budagov,¹⁶ H. S. Budd,⁵⁰ S. Budd,²⁵ K. Burkett,¹⁸ G. Busetto,^{44b,44a} P. Bussey,²² A. Buzatu,³⁴ K. L. Byrum,² S. Cabrera,^{17,y} C. Calancha,³² S. Camarda,⁴ M. Campanelli,³¹ M. Campbell,³⁵ F. Canelli,^{14,18} A. Canepa,⁴⁶ B. Carls,²⁵ D. Carlsmith,⁶⁰ R. Carosi,^{47a} S. Carrillo,^{19,o} S. Carron,¹⁸ B. Casal,¹² M. Casarsa,¹⁸ A. Castro,^{6b,6a} P. Catastini,^{47c,47a} D. Cauz,^{55a} V. Cavaliere,^{47c,47a} M. Cavalli-Sforza,⁴ A. Cerri,²⁹ L. Cerrito,^{31,r} S. H. Chang,²⁸ Y. C. Chen,¹ M. Chertok,⁸ G. Chiarelli,^{47a} G. Chlachidze,¹⁸ F. Chlebana,¹⁸ K. Cho,²⁸ D. Chokheli,¹⁶ J. P. Chou,²³ K. Chung,^{18,p} W. H. Chung,⁶⁰ Y. S. Chung,⁵⁰ T. Chwalek,²⁷ C. I. Ciobanu,⁴⁵ M. A. Ciocci,^{47c,47a} A. Clark,²¹ D. Clark,⁷ G. Compostella,^{44a} M. E. Convery,¹⁸ J. Conway,⁸ M. Corbo,⁴⁵ M. Cordelli,²⁰ C. A. Cox,⁸ D. J. Cox,⁸ F. Crescioli,^{47b,47a} C. Cuenca Almenar,⁶¹ J. Cuevas,^{12,w} R. Culbertson,¹⁸ J. C. Cully,³⁵ D. Dagenhart,¹⁸ M. Datta,¹⁸ T. Davies,²² P. de Barbaro,⁵⁰ S. De Cecco,^{52a} A. Deisher,²⁹ G. De Lorenzo,⁴ M. Dell'Orso,^{47b,47a} C. Deluca,⁴ L. Demortier,⁵¹ J. Deng,^{17,g} M. Deninno,^{6a} M. d'Errico,^{44b,44a} A. Di Canto,^{47b,47a} G. P. di Giovanni,⁴⁵ B. Di Ruzza,^{47a} J. R. Dittmann,⁵ M. D'Onofrio,⁴ S. Donati,^{47b,47a} P. Dong,¹⁸ T. Dorigo,^{44a} S. Dube,⁵³ K. Ebina,⁵⁸ A. Elagin,⁵⁴ R. Erbacher,⁸ D. Errede,²⁵ S. Errede,²⁵ N. Ershaidat,^{45,cc} R. Eusebi,⁵⁴ H. C. Fang,²⁹ S. Farrington,⁴³ W. T. Fedorko,¹⁴ R. G. Feild,⁶¹ M. Feindt,²⁷ J. P. Fernandez,³² C. Ferrazza,^{47d,47a} R. Field,¹⁹ G. Flanagan,^{49,t} R. Forrest,⁸ M. J. Frank,⁵ M. Franklin,²³ J. C. Freeman,¹⁸ I. Furic,¹⁹ M. Gallinaro,⁵¹ J. Galyardt,¹³ F. Garberon,¹¹ J. E. Garcia,²¹ A. F. Garfinkel,⁴⁹ P. Garosi,^{47c,47a} H. Gerberich,²⁵ D. Gerdes,³⁵ A. Gessler,²⁷ S. Giagu,^{52b,52a} V. Giakoumopoulou,³ P. Giannetti,^{47a} K. Gibson,⁴⁸ J. L. Gimmell,⁵⁰ C. M. Ginsburg,¹⁸ N. Giokaris,³ M. Giordani,^{55b,55a} P. Giromini,²⁰ M. Giunta,^{47a} G. Giurgiu,¹ V. Glagolev,¹⁶ D. Glenzinski,¹⁸ M. Gold,³⁸ N. Goldschmidt,¹⁹ A. Golossanov,¹⁸ G. Gomez,¹² G. Gomez-Ceballos,³³ M. Goncharov,³³ O. González,³² I. Gorelov,³⁸ A. T. Goshaw,¹⁷ K. Goulianos,⁵¹ A. Gresele,^{44b,44a} S. Grinstein,⁴ C. Grosso-Pilcher,¹⁴ R. C. Group,¹⁸ U. Grundler,²⁵ J. Guimaraes da Costa,²³ Z. Gunay-Unalan,³⁶ C. Haber,²⁹ S. R. Hahn,¹⁸ E. Halkiadakis,⁵³ B.-Y. Han,⁵⁰ J. Y. Han,⁵⁰ F. Happacher,²⁰ K. Hara,⁵⁶ D. Hare,⁵³ M. Hare,⁵⁷ R. F. Harr,⁵⁹ M. Hartz,⁴⁸ K. Hatakeyama,⁵ C. Hays,⁴³ M. Heck,²⁷ J. Heinrich,⁴⁶ M. Herndon,⁶⁰ J. Heuser,²⁷ S. Hewamanage,⁵ D. Hidas,⁵³ C. S. Hill,^{11,d} D. Hirschbuehl,²⁷ A. Hocker,¹⁸ S. Hou,¹ M. Houlden,³⁰ S.-C. Hsu,²⁹ R. E. Hughes,⁴⁰ M. Hurwitz,¹⁴ U. Husemann,⁶¹ M. Hussein,³⁶ J. Huston,³⁶ J. Incandela,¹¹ G. Introzzi,^{47a} M. Iori,^{52b,52a} A. Ivanov,^{8,q} E. James,¹⁸ D. Jang,¹³ B. Jayatilaka,¹⁷ E. J. Jeon,²⁸ M. K. Jha,^{6a} S. Jindariani,¹⁸ W. Johnson,⁸ M. Jones,⁴⁹ K. K. Joo,²⁸ S. Y. Jun,¹³ J. E. Jung,²⁸ T. R. Junk,¹⁸ T. Kamon,⁵⁴ D. Kar,¹⁹ P. E. Karchin,⁵⁹ Y. Kato,^{42,n} R. Kephart,¹⁸ W. Ketchum,¹⁴ J. Keung,⁴⁶ V. Khotilovich,⁵⁴ B. Kilminster,¹⁸ D. H. Kim,²⁸ H. S. Kim,²⁸ H. W. Kim,²⁸ J. E. Kim,²⁸ M. J. Kim,²⁰ S. B. Kim,²⁸ S. H. Kim,⁵⁶ Y. K. Kim,¹⁴ N. Kimura,⁵⁸ L. Kirsch,⁷ S. Klimenko,¹⁹ K. Kondo,⁵⁸ D. J. Kong,²⁸ J. Konigsberg,¹⁹ A. Korytov,¹⁹ A. V. Kotwal,¹⁷ M. Kreps,²⁷ J. Kroll,⁴⁶ D. Krop,¹⁴ N. Krumnack,⁵ M. Kruse,¹⁷ V. Krutelyov,¹¹ T. Kuhr,²⁷ N. P. Kulkarni,⁵⁹ M. Kurata,⁵⁶ S. Kwang,¹⁴ A. T. Laasanen,⁴⁹ S. Lami,^{47a} S. Lammel,¹⁸ M. Lancaster,³¹ R. L. Lander,⁸ K. Lannon,^{40,v} A. Lath,⁵³ G. Latino,^{47c,47a} I. Lazzizzera,^{44b,44a} T. LeCompte,² E. Lee,⁵⁴ H. S. Lee,¹⁴ J. S. Lee,²⁸ S. W. Lee,^{54,x} S. Leone,^{47a} J. D. Lewis,¹⁸ C.-J. Lin,²⁹ J. Linacre,⁴³ M. Lindgren,¹⁸ E. Lipeles,⁴⁶ A. Lister,²¹ D. O. Litvintsev,¹⁸ C. Liu,⁴⁸ T. Liu,¹⁸ N. S. Lockyer,⁴⁶ A. Loginov,⁶¹ L. Lovas,¹⁵ D. Lucchesi,^{44b,44a} J. Lueck,²⁷ P. Lujan,²⁹ P. Lukens,¹⁸ G. Lungu,⁵¹ J. Lys,²⁹ R. Lysak,¹⁵ D. MacQueen,³⁴ R. Madrak,¹⁸ K. Maeshima,¹⁸ K. Makhoul,³³ P. Maksimovic,¹ S. Malde,⁴³ S. Malik,³¹ G. Manca,^{30,f} A. Manousakis-Katsikakis,³ F. Margaroli,⁴⁹ C. Marino,²⁷ C. P. Marino,²⁵ A. Martin,⁶¹ V. Martin,^{22,1} M. Martínez,⁴ R. Martínez-Ballarín,³² P. Mastrandrea,^{52a} M. Mathis,¹ M. E. Mattson,⁵⁹ P. Mazzanti,^{6a} K. S. McFarland,⁵⁰ P. McIntyre,⁵⁴ R. McNulty,^{30,k} A. Mehta,³⁰ P. Mehtala,²⁴ A. Menzione,^{47a} C. Mesropian,⁵¹ T. Miao,¹⁸ D. Mietlicki,³⁵ N. Miladinovic,⁷ R. Miller,³⁶ C. Mills,²³ M. Milnik,²⁷ A. Mitra,¹ G. Mitselmakher,¹⁹ H. Miyake,⁵⁶ S. Moed,²³ N. Moggi,^{6a} M. N. Mondragon,^{18,o} C. S. Moon,²⁸ R. Moore,¹⁸ M. J. Morello,^{47a} J. Morlock,²⁷ P. Movilla Fernandez,¹⁸ J. Mühlentadt,²⁹ A. Mukherjee,¹⁸ Th. Müller,²⁷ P. Murat,¹⁸ M. Mussini,^{6b,6a} J. Nachtman,^{18,p} Y. Nagai,⁵⁶ J. Naganoma,⁵⁶ K. Nakamura,⁵⁶ I. Nakano,⁴¹ A. Napier,⁵⁷ J. Nett,⁶⁰ C. Neu,^{46,aa} M. S. Neubauer,²⁵ S. Neubauer,²⁷ J. Nielsen,^{29,h} L. Nodulman,² M. Norman,¹⁰ O. Norniella,²⁵ E. Nurse,³¹

L. Oakes,⁴³ S. H. Oh,¹⁷ Y. D. Oh,²⁸ I. Oksuzian,¹⁹ T. Okusawa,⁴² R. Orava,²⁴ K. Osterberg,²⁴ S. Pagan Griso,^{44b,44a} C. Pagliarone,^{55a} E. Palencia,¹⁸ V. Papadimitriou,¹⁸ A. Papaikonomou,²⁷ A. A. Paramanov,² B. Parks,⁴⁰ S. Pashapour,³⁴ J. Patrick,¹⁸ G. Pauletta,^{55b,55a} M. Paulini,¹³ C. Paus,³³ T. Peiffer,²⁷ D. E. Pellett,⁸ A. Penzo,^{55a} T. J. Phillips,¹⁷ G. Piacentino,^{47a} E. Pianori,⁴⁶ L. Pinera,¹⁹ K. Pitts,²⁵ C. Plager,⁹ L. Pondrom,⁶⁰ K. Potamianos,⁴⁹ O. Poukhov,^{16,a} F. Prokoshin,^{16,z} A. Pronko,¹⁸ F. Ptohos,^{18,j} E. Pueschel,¹³ G. Punzi,^{47b,47a} J. Pursley,⁶⁰ J. Rademacker,^{43,d} A. Rahaman,⁴⁸ V. Ramakrishnan,⁶⁰ N. Ranjan,⁴⁹ I. Redondo,³² P. Renton,⁴³ M. Renz,²⁷ M. Rescigno,^{52a} S. Richter,²⁷ F. Rimondi,^{6b,6a} L. Ristori,^{47a} A. Robson,²² T. Rodrigo,¹² T. Rodriguez,⁴⁶ E. Rogers,²⁵ S. Rolli,⁵⁷ R. Roser,¹⁸ M. Rossi,^{55a} R. Rossin,¹¹ P. Roy,³⁴ A. Ruiz,¹² J. Russ,¹³ V. Rusu,¹⁸ B. Rutherford,¹⁸ H. Saarikko,²⁴ A. Safonov,⁵⁴ W. K. Sakumoto,⁵⁰ L. Santi,^{55b,55a} L. Sartori,^{47a} K. Sato,⁵⁶ A. Savoy-Navarro,⁴⁵ P. Schlabach,¹⁸ A. Schmidt,²⁷ E. E. Schmidt,¹⁸ M. A. Schmidt,¹⁴ M. P. Schmidt,^{61,a} M. Schmitt,³⁹ T. Schwarz,⁸ L. Scodellaro,¹² A. Scribano,^{47c,47a} F. Scuri,^{47a} A. Sedov,⁴⁹ S. Seidel,³⁸ Y. Seiya,⁴² A. Semenov,¹⁶ L. Sexton-Kennedy,¹⁸ F. Sforza,^{47b,47a} A. Sfyrila,²⁵ S. Z. Shalhout,⁵⁹ T. Shears,³⁰ P. F. Shepard,⁴⁸ M. Shimojima,^{56,u} S. Shiraishi,¹⁴ M. Shochet,¹⁴ Y. Shon,⁶⁰ I. Shreyber,³⁷ A. Simonenko,¹⁶ P. Sinervo,³⁴ A. Sisakyan,¹⁶ A. J. Slaughter,¹⁸ J. Slaunwhite,⁴⁰ K. Sliwa,⁵⁷ J. R. Smith,⁸ F. D. Snider,¹⁸ R. Snihur,³⁴ A. Soha,¹⁸ S. Somalwar,⁵³ V. Sorin,⁴ P. Squillacioti,^{47c,47a} M. Stanitzki,⁶¹ R. St. Denis,²² B. Stelzer,³⁴ O. Stelzer-Chilton,³⁴ D. Stentz,³⁹ J. Strologas,³⁸ G. L. Strycker,³⁵ J. S. Suh,²⁸ A. Sukhanov,¹⁹ I. Suslov,¹⁶ A. Taffard,^{25,g} R. Takashima,⁴¹ Y. Takeuchi,⁵⁶ R. Tanaka,⁴¹ J. Tang,¹⁴ M. Tecchio,³⁵ P. K. Teng,¹ J. Thom,^{18,i} J. Thome,¹³ G. A. Thompson,²⁵ E. Thomson,⁴⁶ P. Tipton,⁶¹ P. Tito-Guzmán,³² S. Tkaczyk,¹⁸ D. Toback,⁵⁴ S. Tokar,¹⁵ K. Tollefson,³⁶ T. Tomura,⁵⁶ D. Tonelli,¹⁸ S. Torre,²⁰ D. Torretta,¹⁸ P. Totaro,^{55b,55a} S. Tourneur,⁴⁵ M. Trovato,^{47d,47a} S.-Y. Tsai,¹ Y. Tu,⁴⁶ N. Turini,^{47c,47a} F. Ukegawa,⁵⁶ S. Uozumi,²⁸ N. van Remortel,^{24,c} A. Varganov,³⁵ E. Vataga,^{47a,47d} F. Vázquez,^{19,o} G. Velez,¹⁸ C. Vellidis,³ M. Vidal,³² I. Vila,¹² R. Vilar,¹² M. Vogel,³⁸ I. Volobouev,^{29,x} G. Volpi,^{47b,47a} P. Wagner,⁴⁶ R. G. Wagner,² R. L. Wagner,¹⁸ W. Wagner,^{27,bb} J. Wagner-Kuhr,²⁷ T. Wakisaka,⁴² R. Wallny,⁹ S. M. Wang,¹ A. Warburton,³⁴ D. Waters,³¹ M. Weinberger,⁵⁴ J. Weinelt,²⁷ W. C. Wester III,¹⁸ B. Whitehouse,⁵⁷ D. Whiteson,^{46,g} A. B. Wicklund,² E. Wicklund,¹⁸ S. Wilbur,¹⁴ G. Williams,³⁴ H. H. Williams,⁴⁶ P. Wilson,¹⁸ B. L. Winer,⁴⁰ P. Wittich,^{18,i} S. Wolbers,¹⁸ C. Wolfe,¹⁴ H. Wolfe,⁴⁰ T. Wright,³⁵ X. Wu,²¹ F. Würthwein,¹⁰ A. Yagil,¹⁰ K. Yamamoto,⁴² J. Yamaoka,¹⁷ U. K. Yang,^{14,s} Y. C. Yang,²⁸ W. M. Yao,²⁹ G. P. Yeh,¹⁸ K. Yi,^{18,p} J. Yoh,¹⁸ K. Yorita,⁵⁸ T. Yoshida,^{42,m} G. B. Yu,¹⁷ I. Yu,²⁸ S. S. Yu,¹⁸ J. C. Yun,¹⁸ A. Zanetti,^{55a} Y. Zeng,¹⁷ X. Zhang,²⁵ Y. Zheng,^{9,e} and S. Zucchelli^{6b,6a}

(CDF Collaboration)

¹*Institute of Physics, Academia Sinica, Taipei, Taiwan 11529, People's Republic of China*²*Argonne National Laboratory, Argonne, Illinois 60439, USA*³*University of Athens, 157 71 Athens, Greece*⁴*Institut de Física d'Altes Energies, Universitat Autònoma de Barcelona, E-08193, Bellaterra (Barcelona), Spain*⁵*Baylor University, Waco, Texas 76798, USA*^{6a}*Istituto Nazionale di Fisica Nucleare Bologna, I-40127 Bologna, Italy*^{6b}*University of Bologna, I-40127 Bologna, Italy*⁷*Brandeis University, Waltham, Massachusetts 02254, USA*⁸*University of California, Davis, Davis, California 95616, USA*⁹*University of California, Los Angeles, Los Angeles, California 90024, USA*¹⁰*University of California, San Diego, La Jolla, California 92093, USA*¹¹*University of California, Santa Barbara, Santa Barbara, California 93106, USA*¹²*Instituto de Física de Cantabria, CSIC-University of Cantabria, 39005 Santander, Spain*¹³*Carnegie Mellon University, Pittsburgh, Pennsylvania 15213, USA*¹⁴*Enrico Fermi Institute, University of Chicago, Chicago, Illinois 60637, USA*¹⁵*Comenius University, 842 48 Bratislava, Slovakia; Institute of Experimental Physics, 040 01 Kosice, Slovakia*¹⁶*Joint Institute for Nuclear Research, RU-141980 Dubna, Russia*¹⁷*Duke University, Durham, North Carolina 27708, USA*¹⁸*Fermi National Accelerator Laboratory, Batavia, Illinois 60510, USA*¹⁹*University of Florida, Gainesville, Florida 32611, USA*²⁰*Laboratori Nazionali di Frascati, Istituto Nazionale di Fisica Nucleare, I-00044 Frascati, Italy*²¹*University of Geneva, CH-1211 Geneva 4, Switzerland*²²*Glasgow University, Glasgow G12 8QQ, United Kingdom*²³*Harvard University, Cambridge, Massachusetts 02138, USA*²⁴*Division of High Energy Physics, Department of Physics, University of Helsinki and Helsinki Institute of Physics, FIN-00014, Helsinki, Finland*

- ²⁵University of Illinois, Urbana, Illinois 61801, USA
¹The Johns Hopkins University, Baltimore, Maryland 21218, USA
²⁷Institut für Experimentelle Kernphysik, Karlsruhe Institute of Technology, D-76131 Karlsruhe, Germany
²⁸Center for High Energy Physics: Kyungpook National University, Daegu 702-701, Korea;
 Seoul National University, Seoul 151-742, Korea;
 Sungkyunkwan University, Suwon 440-746, Korea;
 Korea Institute of Science and Technology Information, Daejeon 305-806, Korea;
 Chonnam National University, Gwangju 500-757, Korea;
 Chonbuk National University, Jeonju 561-756, Korea
²⁹Ernest Orlando Lawrence Berkeley National Laboratory, Berkeley, California 94720, USA
³⁰University of Liverpool, Liverpool L69 7ZE, United Kingdom
³¹University College London, London WC1E 6BT, United Kingdom
³²Centro de Investigaciones Energeticas Medioambientales y Tecnologicas, E-28040 Madrid, Spain
³³Massachusetts Institute of Technology, Cambridge, Massachusetts 02139, USA
³⁴Institute of Particle Physics: McGill University, Montréal, Québec, Canada H3A 2T8;
 Simon Fraser University, Burnaby, British Columbia, Canada V5A 1S6;
 University of Toronto, Toronto, Ontario, Canada M5S 1A7;
 and TRIUMF, Vancouver, British Columbia, Canada V6T 2A3
³⁵University of Michigan, Ann Arbor, Michigan 48109, USA
³⁶Michigan State University, East Lansing, Michigan 48824, USA
³⁷Institution for Theoretical and Experimental Physics, ITEP, Moscow 117259, Russia
³⁸University of New Mexico, Albuquerque, New Mexico 87131, USA
³⁹Northwestern University, Evanston, Illinois 60208, USA
⁴⁰The Ohio State University, Columbus, Ohio 43210, USA
⁴¹Okayama University, Okayama 700-8530, Japan
⁴²Osaka City University, Osaka 588, Japan
⁴³University of Oxford, Oxford OX1 3RH, United Kingdom
^{44a}Istituto Nazionale di Fisica Nucleare, Sezione di Padova-Trento, I-35131 Padova, Italy
^{44b}University of Padova, I-35131 Padova, Italy
⁴⁵LPNHE, Université Pierre et Marie Curie/IN2P3-CNRS, UMR7585, Paris, F-75252 France
⁴⁶University of Pennsylvania, Philadelphia, Pennsylvania 19104, USA
^{47a}Istituto Nazionale di Fisica Nucleare Pisa, I-56127 Pisa, Italy
^{47b}University of Pisa, I-56127 Pisa, Italy
^{47c}University of Siena, I-56127 Pisa, Italy
^{47d}Scuola Normale Superiore, I-56127 Pisa, Italy
⁴⁸University of Pittsburgh, Pittsburgh, Pennsylvania 15260, USA
⁴⁹Purdue University, West Lafayette, Indiana 47907, USA
⁵⁰University of Rochester, Rochester, New York 14627, USA
⁵¹The Rockefeller University, New York, New York 10021, USA
^{52a}Istituto Nazionale di Fisica Nucleare, Sezione di Roma 1, I-00185 Roma, Italy
^{52b}Sapienza Università di Roma, I-00185 Roma, Italy
⁵³Rutgers University, Piscataway, New Jersey 08855, USA
⁵⁴Texas A&M University, College Station, Texas 77843, USA
^{55a}Istituto Nazionale di Fisica Nucleare Trieste/Udine, I-34100 Trieste, Italy
^{55b}University of Trieste/Udine, I-33100 Udine, Italy
⁵⁶University of Tsukuba, Tsukuba, Ibaraki 305, Japan
⁵⁷Tufts University, Medford, Massachusetts 02155, USA
⁵⁸Waseda University, Tokyo 169, Japan
⁵⁹Wayne State University, Detroit, Michigan 48201, USA
⁶⁰University of Wisconsin, Madison, Wisconsin 53706, USA
⁶¹Yale University, New Haven, Connecticut 06520, USA

(Received 24 November 2009; published 10 March 2010)

We report two complementary measurements of the $WW + WZ$ cross section in the final state consisting of an electron or muon, missing transverse energy, and jets, performed using $p\bar{p}$ collision data at $\sqrt{s} = 1.96$ TeV collected by the CDF II detector. The first method uses the dijet invariant mass distribution while the second more sensitive method uses matrix-element calculations. The result from the second method has a signal significance of 5.4σ and is the first observation of $WW + WZ$ production using this signature. Combining the results gives $\sigma_{WW+WZ} = 16.0 \pm 3.3$ pb, in agreement with the standard model prediction.

DOI: 10.1103/PhysRevLett.104.101801

PACS numbers: 14.70.Fm, 12.15.Ji, 14.70.Hp, 14.80.Bn

Measurements involving heavy vector boson pairs (WW , WZ , and ZZ) are important tests of the electroweak sector of the standard model. Deviations of the production cross section from predictions could arise from anomalous triple gauge boson interactions [1] or from new resonances decaying to vector bosons. Furthermore, the topology of diboson events is similar to that of events in which a Higgs boson is produced in association with a W or a Z , allowing diboson measurements to provide an important step towards future measurements of Higgs boson production.

Diboson production has been observed at the Tevatron in channels in which both bosons decay leptonically [2,3]. Extraction of the diboson signal in hadronic channels is more challenging because of significantly larger backgrounds. In addition, due to limited detector resolution, it is difficult to distinguish hadronically decaying W bosons from Z bosons. We report on two measurements of the cross section, $\sigma(p\bar{p} \rightarrow WW + WZ)$, with the CDF II detector [4] that use different techniques applied to the leptonic decay of one W and the hadronic decay of the associated W or Z ($WW/WZ \rightarrow \ell\nu qq$, where ℓ represents a high- p_T electron or muon). Our result represents the first observation of this signal in the lepton + jets channel. Evidence has previously been reported by the D0 Collaboration [5], and the CDF Collaboration set a limit on its cross section times branching ratio [6]. In addition, the CDF Collaboration has reported observation of $WW + WZ + ZZ$ in a different hadronic channel with large missing transverse energy and jets [7].

The first method uses the invariant mass of the two-jet system (M_{jj}) to extract a signal peak from data corresponding to 3.9 fb^{-1} of $p\bar{p}$ collisions at $\sqrt{s} = 1.96 \text{ TeV}$. The second method takes advantage of more kinematic information in the event by constructing a discriminant based on calculations of the differential cross sections of the signal and background processes. This so-called matrix-element (ME) method has been employed in a search for a low-mass Higgs produced in association with a W boson [8] and in a measurement of single top production [9]. It is expected to achieve greater discriminating power and here uses data corresponding to an integrated luminosity of 2.7 fb^{-1} .

Data samples common to both analyses use trigger selections requiring a central electron (muon) with E_T (p_T) $> 18 \text{ GeV}$. The ME method utilizes an additional sample derived from a trigger requiring two jets and large missing transverse energy (\cancel{E}_T) [10].

Off-line we select events with electron (muon) candidates with E_T (p_T) $> 20 \text{ GeV}$, and with \cancel{E}_T , jet, and other kinematic requirements chosen differently for the two methods. Jets are clustered using a fixed-cone algorithm with radius $\Delta R = \sqrt{(\Delta\eta)^2 + (\Delta\phi)^2} = 0.4$ and their energies are corrected for detector effects [11]. Cosmic ray

and photon conversion candidates are identified and removed.

Further event selection requirements are made to reduce backgrounds and the sensitivity to systematic uncertainties. In the M_{jj} method, we require events to have $\cancel{E}_T > 25 \text{ GeV}$, at least two jets with $E_T > 15 \text{ GeV}$ and $|\eta| < 2.4$, and the dijet vector boson candidate to have $p_T > 40 \text{ GeV}/c$. As a result of these selection criteria, the M_{jj} distribution for background is smoothly falling in the region where the signal is expected to peak. The invariant mass of the dijet vector boson candidate, M_{jj} , is evaluated from the two most energetic jets. Additional requirements are made to reduce backgrounds and improve the Monte Carlo modeling of event kinematics: the transverse mass of the lepton and \cancel{E}_T system [$M_T(W)$] [10] must be greater than $30 \text{ GeV}/c^2$, and the two most energetic jets must be separated by $|\Delta\eta| < 2.5$.

In the ME method, we require events to have $\cancel{E} > 20 \text{ GeV}$ and exactly two jets with $E_T > 25 \text{ GeV}$ and $|\eta| < 2.0$. Additional selection criteria to reduce backgrounds and achieve good modeling of the quantities used in the matrix-element calculation include the rejection of events with either an additional jet of $E_T > 12 \text{ GeV}$ or a second high- p_T charged lepton. The latter reduces $Z + \text{jets}$, $t\bar{t}$, and leptonic diboson backgrounds. For events with an electron candidate, there is a significant background from production of multiple jets (multijet in the following) by quantum chromodynamical (QCD) processes, where the electron is faked by a hadronic jet. The ME method deals with this background by applying stringent selection criteria, while the M_{jj} method assigns a systematic uncertainty to the background shape. The reduction of the multijet QCD background in the ME analysis is achieved by raising the \cancel{E}_T cut to 40 GeV , requiring $M_T(W) > 70 \text{ GeV}/c^2$, and imposing additional cuts on the angles between the jets, the lepton, and the \cancel{E}_T [12]. There is a less stringent requirement of $M_T(W) > 10 \text{ GeV}/c^2$ imposed on muon events to reduce the QCD background in that channel.

After these selections for both methods, the dominant background to the diboson signal is a W boson produced with accompanying jets ($W + \text{jets}$), where the W decays leptonically. Smaller but non-negligible backgrounds come from QCD multijet (where one jet mimics a lepton signature), $Z + \text{jets}$, $t\bar{t}$, and single top production. QCD multijet events are modeled using data with loosened lepton selection criteria. Signal and other background processes are modeled using event generators and a GEANT-based CDF II detector simulation. The diboson signals and the $t\bar{t}$ and single top backgrounds are simulated using the PYTHIA event generator [13]. The $W + \text{jets}$ and $Z + \text{jets}$ backgrounds are simulated using the tree-level event generator ALPGEN [14], with an interface to PYTHIA providing parton showering and hadronization.

The normalization of the $Z + \text{jets}$ background is based on the measured cross section while for $t\bar{t}$ and single top backgrounds the next-to-leading order predicted cross section is used [15]. The efficiencies for the $Z + \text{jets}$, $t\bar{t}$, and single top backgrounds are estimated from simulation. The normalization of the QCD background is estimated by fitting the \cancel{E}_T spectrum in data to the sum of all contributing processes, where the QCD and $W + \text{jets}$ normalizations float in the fit. In the final signal extractions from both methods, the multijet QCD background is Gaussian constrained to the result of this \cancel{E}_T fit and the $W + \text{jets}$ background is left unconstrained.

We now describe the methodology and results from each technique. In the M_{jj} method we extract the signal fraction from the data by performing a χ^2 fit to the dijet invariant mass spectrum separately for electron and muon events. Templates of M_{jj} distributions are constructed with the multijet QCD background, the signal $WW + WZ$ processes, and the sum of the electroweak backgrounds ($Z + \text{jets}$, $W + \text{jets}$, and $t\bar{t}$ production).

Figure 1 shows the fit results superimposed on data after the electron and muon samples are combined. Also shown is the data M_{jj} distribution after having subtracted the estimated background, superimposed on the signal model normalized to the fit result. Combining the two χ^2 fit results we get a total of $1079 \pm 232(\text{stat}) \pm 86(\text{syst})$ $WW/WZ \rightarrow \ell\nu jj$ events, of which about 60% are muon events and 40% are electron events. The observed significance is 4.6σ where 4.9σ is expected. The resultant $WW + WZ$ production cross section measurement is

$\sigma_{WW+WZ} = 14.4 \pm 3.1(\text{stat}) \pm 2.2(\text{syst})$ pb. The sources of systematic uncertainty in this measurement are discussed together with those from the ME method below.

In the ME method a probability density $P(x)$ that an event was produced by a given process is determined using the standard model differential cross section for that process. For an event with measured quantities x , we integrate the appropriate differential cross section $d\sigma(y)$ over the partonic quantities y convolved with the parton distribution functions (PDFs) and a transfer function:

$$P(x) = \frac{1}{\sigma} \int d\sigma(y) dq_1 dq_2 f(q_1) f(q_2) W(y, x). \quad (1)$$

The PDFs [$f(q_1)$ and $f(q_2)$] are evaluated according to the CTEQ5L parametrization [16]. The transfer function $W(x, y)$ relates x to y , encoding the effects of the detector resolution. The momenta of electrons, muons, and the angles of jets are assumed to be measured exactly and a mapping of measured jet energy to partonic energy is derived using the full detector simulation. The integration is performed over the energy of the partons and the longitudinal momentum of the neutrino. The matrix element is calculated with tree-level diagrams from MADGRAPH [17]. Event probability densities are calculated for the signal processes as well as for $W + \text{jets}$ and single top background processes. The event probabilities are combined into an event probability discriminant: $\text{EPD} = P_{\text{signal}} / (P_{\text{signal}} + P_{\text{background}})$, where $P_{\text{signal}} = P_{WW} + P_{WZ}$ and $P_{\text{background}} = P_{W+\text{jets}} + P_{\text{single top}}$. We make templates of the EPD for all signal and background processes and ultimately extract the signal using a fit of the observed EPD distribution to a sum of the templates. The expected event yields are as shown in Table I for the ME method's event selection.

Figure 2 shows the dijet mass in bins of EPD. Most of the background events have low EPD. Events with $\text{EPD} > 0.25$ have a dijet mass peak close to the expected W/Z resonance, and the signal-to-background ratio improves with increasing EPD.

Before comparing the observed EPD to the prediction, we validate the Monte Carlo modeling of the quantities that

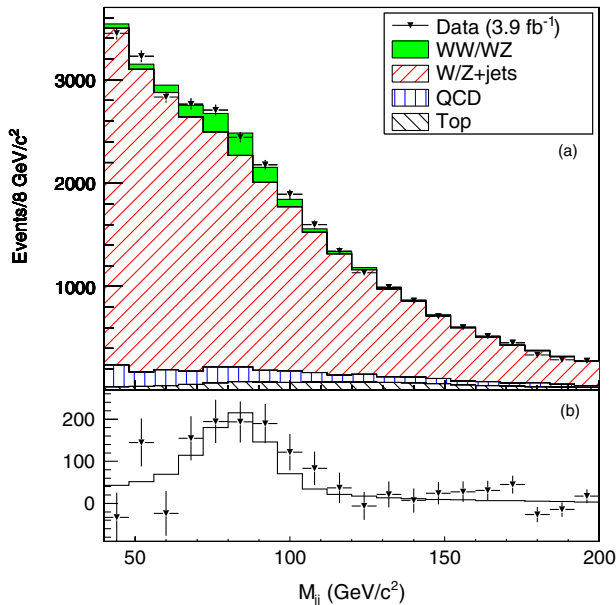


FIG. 1 (color online). Dijet invariant mass distribution of reconstructed $W/Z \rightarrow jj$ candidates compared to the fitted signal and background components (a), and for the corresponding background subtracted distribution (b).

TABLE I. Expected and observed event yields after the ME method selection in 2.7 fb^{-1} of data.

Process	Predicted event yield
WW signal	446 ± 29
WZ signal	79 ± 6
$W + \text{jets}$	$10\,175 \pm 305$
$Z + \text{jets}$	584 ± 88
QCD multijet	283 ± 113
$t\bar{t} + \text{single top}$	241 ± 29
Observed	11 812

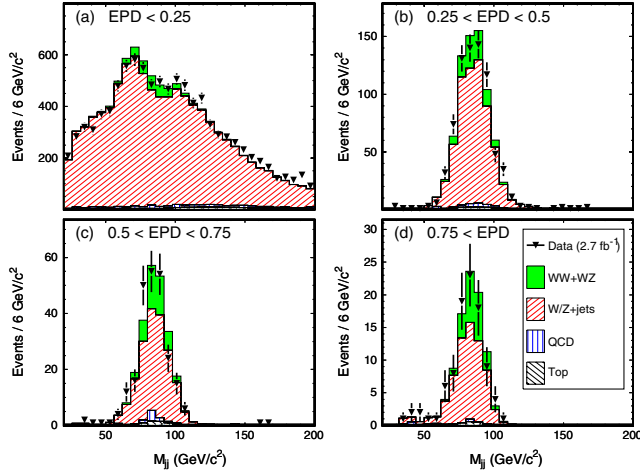


FIG. 2 (color online). M_{jj} for events with (a) $\text{EPD} < 0.25$, (b) $0.25 < \text{EPD} < 0.5$, (c) $0.5 < \text{EPD} < 0.75$, and (d) $\text{EPD} > 0.75$.

enter the matrix-element calculation. We compare the observed distributions to the predicted ones in control regions with very little signal and also in the signal-rich region. The different regions are chosen according to the invariant mass of the two-jet system (M_{jj}): the signal-rich region has $55 < M_{jj} < 120$ GeV and the control regions cover the rest of the M_{jj} range. We also check the modeling of the properties (mass, p_T , and η) of the leptonic W boson and the hadronic W or Z boson candidate. All of these quantities are well described by the simulation for our event selection. There is a small discrepancy in the description of M_{jj} in the control regions, as is visible in the low-EPD region of Fig. 2. Associated with this discrepancy we assign a systematic mismodeling uncertainty which is derived in the control regions and extrapolated through the signal region. This uncertainty has a negligible effect on the results, because most background events lie in the first few bins of the EPD distribution. Small changes in modeling of those background events do not change the shape of the EPD.

The observed and predicted EPDs are shown in Fig. 3. We use a binned-likelihood fit of the observed EPD to a sum of templates, testing both a background-only hypothesis and a signal-plus-background ($s + b$) hypothesis. Systematic uncertainties, discussed further below, are included in the fit as constrained parameters. We perform pseudoexperiments to calculate the probability (p value) that the background-only discriminant fluctuates up to the observed result (observed p value) and up to the median expected $s + b$ result (expected p value). We observe a p value of 2.1×10^{-7} , corresponding to a signal significance of 5.4σ , where 5.1σ is expected. The observed $WW + WZ$ cross section is $\sigma_{WW+WZ} = 17.7 \pm 3.1(\text{stat}) \pm 2.4(\text{syst})$ pb.

We consider several sources of systematic uncertainty in both methods, taking into account their effect on both

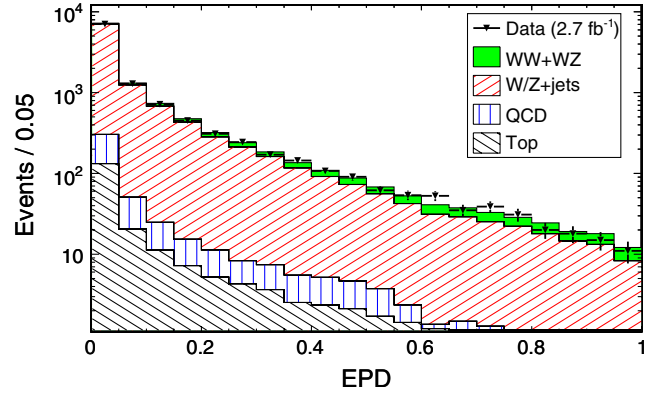


FIG. 3 (color online). Observed EPD distribution superimposed on distribution expected from simulated processes.

the signal acceptance and the shape of the background and signal templates. The uncertainty on the normalization of the backgrounds is taken as part of the statistical uncertainty. In the M_{jj} method the largest systematic uncertainties are due to the modeling of the electroweak and QCD shapes, about 8% and 6%, respectively. In the ME method the uncertainty in the jet energy scale is the largest systematic uncertainty, at about 10%, which includes contributions both from the signal acceptance and from the shapes of the signal templates. In the M_{jj} method this uncertainty is about 6%. Both methods include an uncertainty of about 5% due to initial and final state radiation and a 6% uncertainty on the integrated luminosity. Smaller contributions arise from PDFs, jet energy resolution, the factorization and renormalization scales used in the $W + \text{jets}$ simulation, and trigger and lepton identification efficiencies.

One measure of how the two methods are correlated is the expected overlap of $WW + WZ$ signal. Accounting for the different integrated luminosities used, 15% of the signal in the M_{jj} analysis is common to that in the EPD analysis. Conversely, 29% of the signal in the EPD analysis is common to that in the M_{jj} analysis. This corresponds to a statistical correlation of about 21%. If we assume the systematic uncertainties are 100% correlated, then the total correlation between the two analyses is 49%, leading to a combined [18] result of $\sigma_{WW+WZ} = 16.0 \pm 3.3(\text{stat} + \text{syst})$ pb. Because the total uncertainties on the two input measurements are similar, the combined central value does not depend significantly on the correlation assumed. The total uncertainty in the combined result increases with increasing correlation and we quote the value assuming maximum possible correlation. The signal overlap with the CDF $WW + WZ + ZZ$ observation in the $\cancel{E}_T + \text{jets}$ channel [7] is also studied. While that analysis requires much larger \cancel{E}_T , it does not veto events with identified leptons. We found that about 15% of the $WW + WZ$ signal from the $\cancel{E}_T + \text{jets}$ analysis appears in the analyses presented here.

In summary, we observe $WW + WZ$ production in the lepton plus jets plus \cancel{E}_T final state. We perform two searches: one seeking a resonance on top of a smoothly falling dijet mass distribution, and another building a discriminant using a matrix-element technique. The combined $WW + WZ$ cross section from these two methods is measured to be $\sigma_{WW+WZ} = 16.0 \pm 3.3(\text{stat} + \text{syst})$ pb, in good agreement with the prediction of 16.1 ± 0.9 pb [19]. Measurements of these diboson processes are tests of electroweak theory and a necessary step toward validating Higgs boson search techniques at the Tevatron.

We thank the Fermilab staff and the technical staffs of the participating institutions for their vital contributions. This work was supported by the U.S. Department of Energy and National Science Foundation; the Italian Istituto Nazionale di Fisica Nucleare; the Ministry of Education, Culture, Sports, Science and Technology of Japan; the Natural Sciences and Engineering Research Council of Canada; the National Science Council of the Republic of China; the Swiss National Science Foundation; the A.P. Sloan Foundation; the Bundesministerium für Bildung und Forschung, Germany; the World Class University Program, the National Research Foundation of Korea; the Science and Technology Facilities Council and the Royal Society, United Kingdom; the Institut National de Physique Nucleaire et Physique des Particules/CNRS; the Russian Foundation for Basic Research; the Ministerio de Ciencia e Innovación, and Programa Consolider-Ingenio 2010, Spain; the Slovak R&D Agency; and the Academy of Finland.

^aDeceased.

^bVisitor from University of Massachusetts Amherst, Amherst, Massachusetts 01003, USA.

^cVisitor from Universiteit Antwerpen, B-2610 Antwerp, Belgium.

^dVisitor from University of Bristol, Bristol BS8 1TL, United Kingdom.

^eVisitor from Chinese Academy of Sciences, Beijing 100864, China.

^fVisitor from Istituto Nazionale di Fisica Nucleare, Sezione di Cagliari, 09042 Monserrato (Cagliari), Italy.

^gVisitor from University of California Irvine, Irvine, CA 92697, USA.

^hVisitor from University of California Santa Cruz, Santa Cruz, CA 95064, USA.

ⁱVisitor from Cornell University, Ithaca, NY 14853, USA.

^jVisitor from University of Cyprus, Nicosia CY-1678, Cyprus.

^kVisitor from University College Dublin, Dublin 4, Ireland.

^lVisitor from University of Edinburgh, Edinburgh EH9 3JZ, United Kingdom.

^mVisitor from University of Fukui, Fukui City, Fukui Prefecture, Japan 910-0017.

ⁿVisitor from Kinki University, Higashi-Osaka City, Japan 577-8502.

^oVisitor from Universidad Iberoamericana, Mexico D.F., Mexico.

^pVisitor from University of Iowa, Iowa City, IA 52242, USA.

^qVisitor from Kansas State University, Manhattan, KS 66506, USA.

^rVisitor from Queen Mary, University of London, London, E1 4NS, United Kingdom.

^sVisitor from University of Manchester, Manchester M13 9PL, United Kingdom.

^tVisitor from Muons, Inc., Batavia, IL 60510, USA.

^uVisitor from Nagasaki Institute of Applied Science, Nagasaki, Japan.

^vVisitor from University of Notre Dame, Notre Dame, IN 46556, USA.

^wVisitor from University de Oviedo, E-33007 Oviedo, Spain.

^xVisitor from Texas Tech University, Lubbock, TX 79609, USA.

^yVisitor from IFIC(CSIC-Universitat de Valencia), 56071 Valencia, Spain.

^zVisitor from Universidad Tecnica Federico Santa Maria, 110v Valparaiso, Chile.

^{aa}Visitor from University of Virginia, Charlottesville, VA 22906, USA.

^{bb}Visitor from Bergische Universität Wuppertal, 42097 Wuppertal, Germany.

^{cc}Visitor from Yarmouk University, Irbid 211-63, Jordan.

^{dd}On leave from J. Stefan Institute, Ljubljana, Slovenia.

- [1] K. Hagiwara, S. Ishihara, R. Szalapski, and D. Zeppenfeld, *Phys. Rev. D* **48**, 2182 (1993).
- [2] D. Acosta *et al.* (CDF Collaboration), *Phys. Rev. Lett.* **94**, 211801 (2005); A. Abulencia *et al.* (CDF Collaboration), *ibid.* **98**, 161801 (2007); T. Aaltonen *et al.* (CDF Collaboration), *ibid.* **100**, 201801 (2008).
- [3] V.M. Abazov *et al.* (D0 Collaboration), *Phys. Rev. Lett.* **94**, 151801 (2005); *Phys. Rev. D* **76**, 111104 (2007).
- [4] D. Acosta *et al.* (CDF Collaboration), *Phys. Rev. D* **71**, 032001 (2005).
- [5] V.M. Abazov *et al.* (D0 Collaboration), *Phys. Rev. Lett.* **102**, 161801 (2009).
- [6] T. Aaltonen *et al.* (CDF Collaboration), *Phys. Rev. D* **79**, 112011 (2009).
- [7] T. Aaltonen *et al.* (CDF Collaboration), *Phys. Rev. Lett.* **103**, 091803 (2009).
- [8] T. Aaltonen *et al.* (CDF Collaboration), *Phys. Rev. Lett.* **103**, 101802 (2009).
- [9] T. Aaltonen *et al.* (CDF Collaboration), *Phys. Rev. Lett.* **101**, 252001 (2008); T. Aaltonen *et al.* (CDF Collaboration), *Phys. Rev. Lett.* **103**, 092002 (2009).
- [10] We use a cylindrical coordinate system with its origin in the center of the detector, where θ and ϕ are the polar and azimuthal angles, respectively, and pseudorapidity is $\eta = -\text{Intan}(\theta/2)$. The transverse momentum of a charged particle is $p_T = p \sin\theta$, where p is the momentum of the charged particle track. The transverse energy, $E_T = E \sin\theta$, is measured using the calorimeter. The missing E_T

- ($\vec{\cancel{E}}_T$) is defined by $\vec{\cancel{E}}_T = -\sum_i E_T^i \hat{n}_i$, where \hat{n}_i is a unit vector perpendicular to the beam axis and pointing at the i th calorimeter tower. $\vec{\cancel{E}}_T$ is corrected for high-energy muons and jet energy corrections. We define $\cancel{E}_T = |\vec{\cancel{E}}_T|$. The transverse mass of the W is defined as $M_T(W) = \sqrt{2p_T^l \cancel{E}_T [1 - \cos(\Delta\phi^{lv})]}$.
- [11] A. Bhatti *et al.*, Nucl. Instrum. Methods Phys. Res., Sect. A **566**, 375 (2006).
- [12] P. Dong, Ph.D. thesis, University of California, Los Angeles [Report No. FERMILAB-THESIS-2008-12, 2008].
- [13] T. Sjöstrand *et al.*, Comput. Phys. Commun. **135**, 238 (2001).
- [14] M.L. Mangano *et al.*, J. High Energy Phys. 07 (2003) 001.
- [15] D. Acosta *et al.* (CDF Collaboration), Phys. Rev. Lett. **94**, 091803 (2005); M. Cacciari *et al.*, J. High Energy Phys. 09 (2008) 127; B.W. Harris *et al.*, Phys. Rev. D **66**, 054024 (2002).
- [16] J. Pumplin *et al.*, J. High Energy Phys. 07 (2002) 012.
- [17] F. Maltoni and T. Stelzer, J. High Energy Phys. 02 (2003) 027.
- [18] L. Lyons, D. Gibaut, and P. Clifford, Nucl. Instrum. Methods Phys. Res., Sect. A **270**, 110 (1988).
- [19] J.M. Campbell and R.K. Ellis, Phys. Rev. D **60**, 113006 (1999).